

Supporting Information

for

Multiplexed Ratiometric Photoluminescent Detection of Pyrophosphate by Anisotropic Boron-doped Nitrogen-rich Carbon Rugby-like Nanodots

Zhong-Xia Wang, Xian-He Yu, Feng Li, Fen-Ying Kong, Wei-Xin Lv and Wei
Wang*

School of Chemistry and Chemical Engineering, Yancheng Institute of Technology,

Yancheng 224051, China.

Corresponding author

*E-mail: wangw@ycit.edu.cn

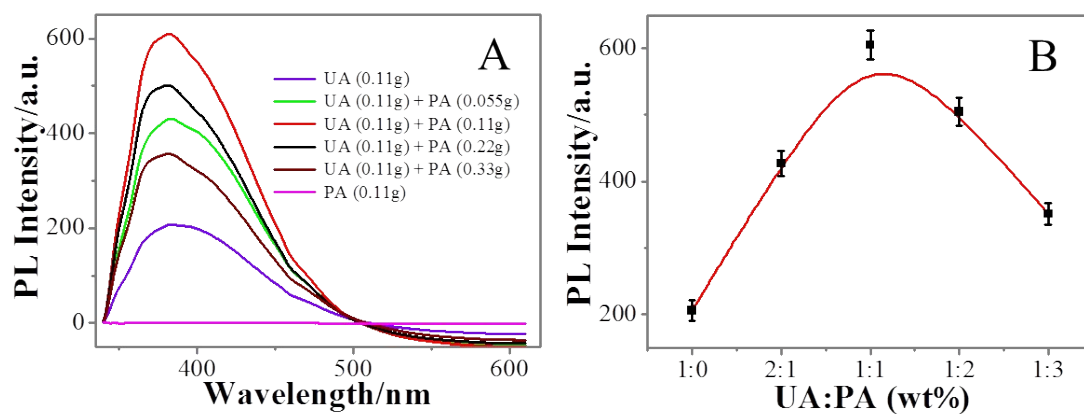


Figure S1 Effect of PA content on the PL maximum emission intensity of the BNCRDs at 370 nm.

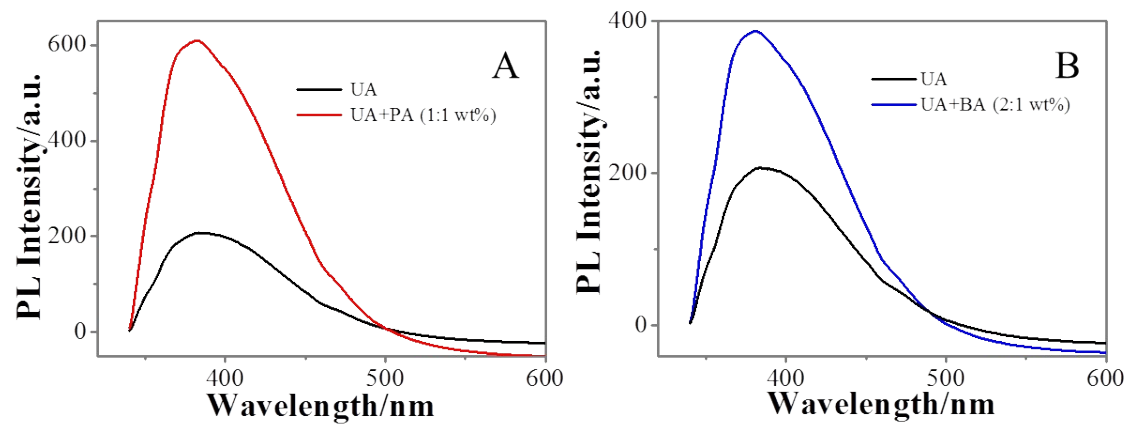


Figure S2 PL spectra of carbon nanomaterials using different comonomers in the precursor solution.

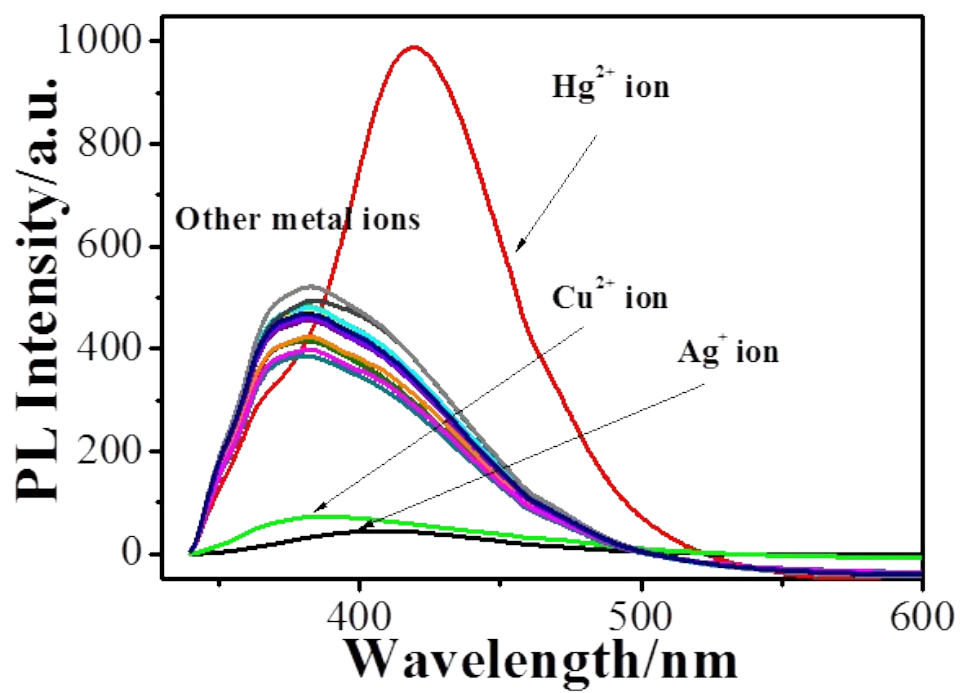


Figure S3 Selectivity of the prepared BNCRDs for detection metal ion system, the concentration of metal ion is 100 μ M.

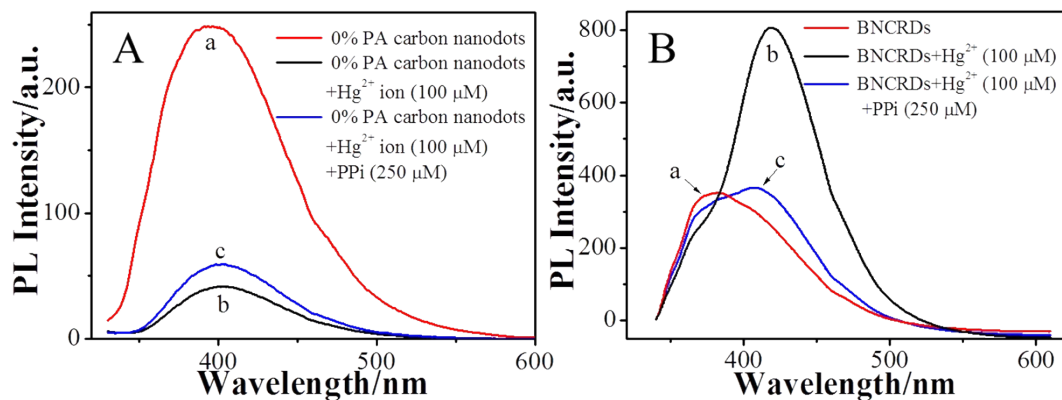


Figure S4 A) PL emission spectrum ($\lambda_{\text{ex}} = 320 \text{ nm}$) of free 0% PA carbon nanodots (curve a), and 0% PA carbon nanodots in the presence of Hg^{2+} ions (curve b), or both Hg^{2+} ions and PPI (curve c); B) PL emission spectrum ($\lambda_{\text{ex}} = 320 \text{ nm}$) of BNCRDs (curve a), and BNCRDs in the presence of Hg^{2+} ions (curve b), or both Hg^{2+} ions and PPI (curve c).

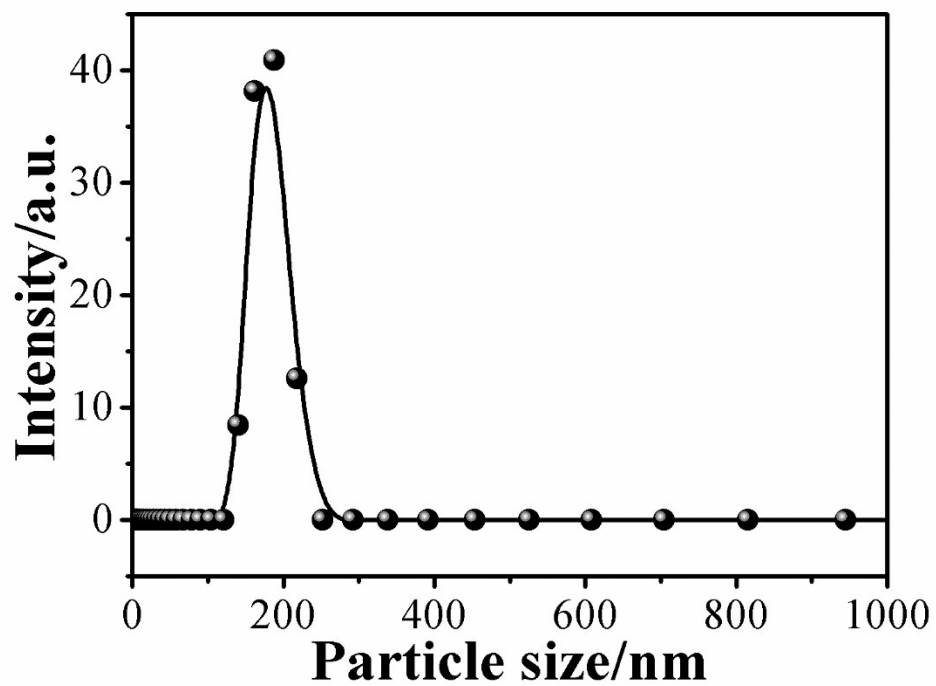


Figure S5 DLS curve of the obtained BNCRDs.

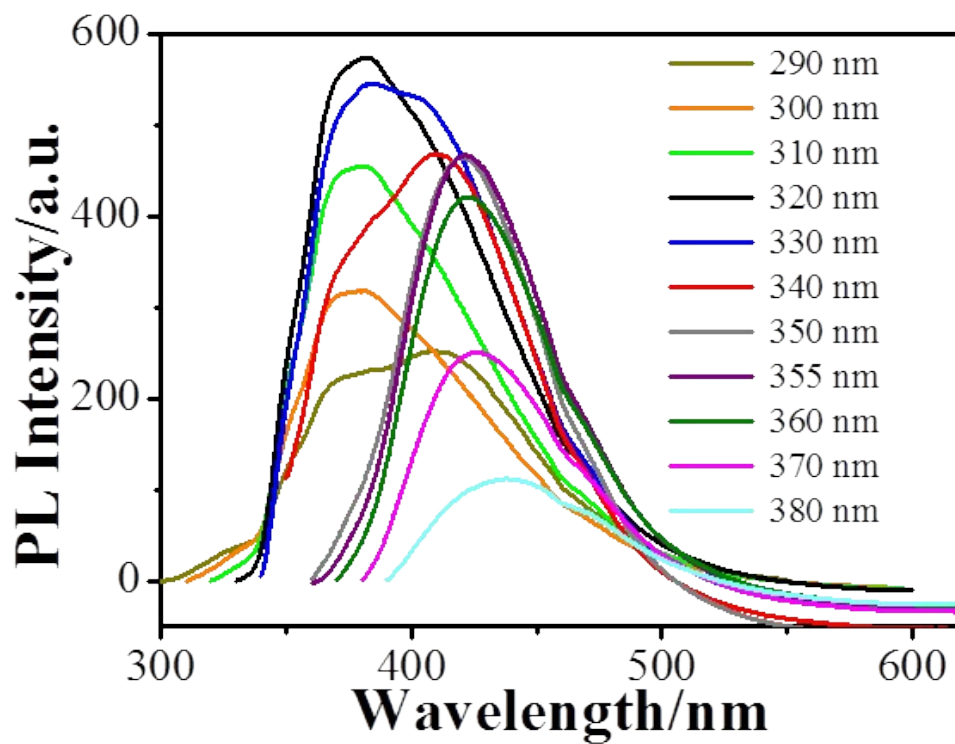


Figure S6 PL spectrum of the BNCRDs at different excitation wavelengths from 290 to 380 nm; both the excitation and emission slit widths were 3 nm.

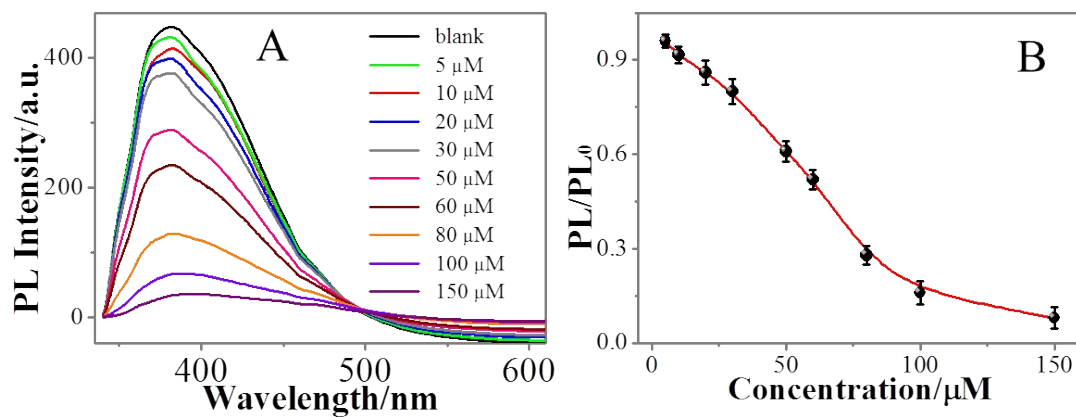


Figure S7 A) PL emission spectra of BNCRDs in the presence of different concentrations of Cu^{2+} ions (0 to 150.0 μM , top to bottom, excitation at 320 nm). B) Plot of the enhanced PL signals PL/PL_0 versus Cu^{2+} ions concentration.

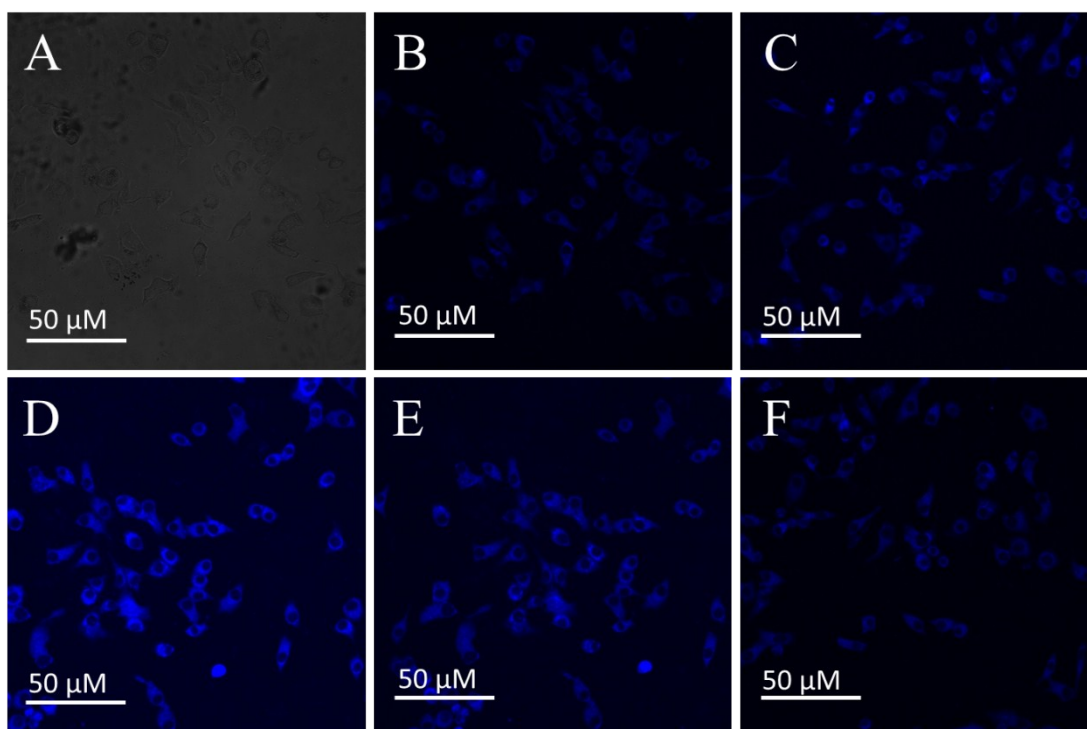


Figure S8 Bright field images (A) and confocal fluorescence images (B) of HeLa cells upon 5.5 h incubation with BNCRDs. Confocal fluorescence images of HeLa cells treated with 40 μM and 80 μM Hg^{2+} ion for 30 min, respectively (C-D). (E-F) Confocal fluorescence image after further incubation with 150 μM and 250 μM PPI for 30 min, respectively. Fluorescence images were taken with 350 nm excitation.

Table S1: Effect of the mass of PA in the precursor solution on the average lifetime of obtained BNCRDs.

UA:PA (wt%)	1:0	2:1	1:1	1:2	1:3
Average lifetime (ns)	3.0749	2.0696	1.4615	1.2100	1.3099

Table S2: FL lifetimes of the BNCRDs, BNCRDs-Hg²⁺ complexes and the BNCRDs-Hg²⁺ complexes in the presence of PPI. Hg²⁺ ions: 100 μM; PPI: 100 μM.

Sample	τ_1/ns (%) ^a	τ_2/ns (%) ^a	RSD (%)
BNCRDs	1.6287 (49.04)	5.8727 (50.96)	3.75
BNCRDs-Hg ²⁺	2.0092 (37.54)	6.2320 (62.46)	3.29
BNCRDs-Hg ²⁺ -PPI	1.4894 (31.31)	4.9758 (68.69)	4.16

^aThe data were obtained from three parallel samples.

Table S3: Comparison of the linear range and detect limit for PPI using different fluorescent probes.

Anions	Method	Linear range	Detect limit	Reference
PPi	Based on poly(phenylene-ethynylene)	0-10 μM	340 nM	[1]
PPi	Based on BSA/MPA-AuNCs	0.4-16 μM	Not given	[2]
PPi	Based on DNA/Ag NCs	0.25 to 10 μM	112.69 nM	[3]
PPi	Based on Au NPs	Not given	\sim 0.5 μM	[4]
PPi	Based on PEI-capped UCNPs	0.5-8.0 μM	184 nM	[5]
PPi	This method	50 nM-280 μM	21.27 nM	Our method
PPi	This method	10 nM-100 μM	4.59 nM	Our method

References:

- [1] X. Zhao, K.S. Schanze, *Chem. Commun.* **2010**, 46, 6075-6077.
- [2] H. H. Deng, F. F. Wang, X. Q. Shi, H. P. Peng, A. L. Liu, X. H. Xia, *Biosens. Bioelectron.* **2016**, 83, 1-8.
- [3] J. L. Ma, B. C. Yin, X. Wu, B. C. Ye, *Anal. Chem.* **2016**, 88, 9219-9225.
- [4] M. Li, J. Li, H. Di, H. Liu, D. Liu, *Anal. Chem.* **2017**, 89, 3532-3537.
- [5] F. Wang, C. Zhang, Q. Xue, H. Li, Y. Xian, *Biosens. Bioelectron.* **2017**, 95, 21-26.